16th Australasian Fluid Mechanics Conference
Crown Plaza, Gold Coast, Australia
2-7 December 2007

Universal regimes of a free turbulent jet

D. V. Strunin

Department of Mathematics and Computing
University of Southern Queensland, Queensland, 4350 AUSTRALIA

Abstract

We apply the K-ε model to analyse the expansion of a free turbulent jet. Due to nonlinearity of turbulent diffusion the model leads to spatially confined solutions (solutions with finite support). We seek the turbulent energy, dissipation and momentum as power series in spatial coordinate across the jet with time-dependent coefficients. The coefficients obey a dynamical system containing slow and fast variables. We show, with the help of numerical analysis, that there exists an attractor for trajectories of the dynamical system, based on a few slow variables.

Introduction

The literature on turbulent jets is extensive and spans over decades [1, 9, 3]. As in other areas of mechanics, special interest present attracting regimes, however, this aspect of the jet dynamics has not received as close attention as, for example, analysis of the structure of pulsations. A self-similar attracting regime of an instantaneous jet, based on the relatively rough K-ℓ model, was obtained in [8]. In the present paper we analyse the K-ε model. We again look for universality, however, from a different angle. Namely, we treat the governing equations as dynamical system and look for attractors of trajectories.

Consider a turbulent jet, which is statistically uniform in horizontal direction and expands freely in an unbounded motionless fluid. The source of turbulence can be, for example, a short impulse in the shape of a narrow plane layer. The velocity shear between the jet and surrounding fluid generates the turbulent kinetic energy K. In the long-term, the turbulent energy decays due to the expansion and due to the loss into heat. The latter loss is expressed by the volume energy dissipation rate ε.

The expansion is driven by the turbulent diffusion which is essentially nonlinear. As a consequence, there is a sharp boundary—front—between the jet and surrounding fluid. We illustrate this property with an example of a single diffusion equation with the diffusion coefficient depending on the unknown function [10] (for other examples see, e.g, handbook [6]). The equation $\partial_t f = \partial_x(f\partial_x f)$ leads to the well-known (similarity) solution $f(x,t) = \alpha t^{-1/3}\left(1-\beta x^2 t^{-2/3}\right)$, where α and β are constants. The point in space where $f(x,t)$ turns into zero defines the position of the front: $1-\beta x^2 t^{-2/3} = 0$ gives $x = h(t) = t^{1/3}\sqrt{\beta}$. Importantly, with α, β fixed, the solution attracts a whole class of solutions evolving from different initial conditions.

We use the K–ε model [5, 4] to describe the dynamics of the turbulent energy, its dissipation rate and momentum:

$$\begin{aligned}
\partial_t K &= \alpha_1 \partial_x\left(\frac{K^2}{\varepsilon}\partial_x K\right) + \alpha_2 \frac{K^2}{\varepsilon}(\partial_x u)^2 - \alpha_3\varepsilon\,,\\
\partial_t \varepsilon &= \beta_1 \partial_x\left(\frac{K^2}{\varepsilon}\partial_x \varepsilon\right) + \beta_2 K(\partial_x u)^2 - \beta_3\frac{\varepsilon^2}{K}\,,\\
\partial_t u &= \chi\partial_x\left(\frac{K^2}{\varepsilon}\partial_x u\right)\,.
\end{aligned} \tag{1}$$

The coordinate x is directed across the turbulent layer starting in its middle. The layer is plane, and infinite and uniform in the y and z directions. $\alpha_{1,2,3}$, $\beta_{1,2,3}$ and χ are positive non-dimensional constants. The system (1) is non-dimensional, obtained from the dimensional one by using some useful scales, for example, the average initial velocity across the jet, U, as the velocity scale; the initial width of the jet, $2h$, as the length scale; U^2 as the turbulent energy scale; U^3/h as the dissipation rate scale; and h/U as the time scale.

The initial conditions for K, ε and u across the jet are supposed to have dome-like shapes with finite support. We assume that they are symmetric with respect to the middle plane. On the turbulent front, $x = h(t)$, the functions $K(x,t)$, $\varepsilon(x,t)$ and $u(x,t)$ are equal to zero and remain zero beyond the front, for $x > h(t)$.

Turbulent jet as dynamical system

We look for solutions of (1) in the form of power series

$$\begin{aligned}
K &= A(t)\left[1 - B_2(t)x^2 - B_4(t)x^4 - B_6(t)x^6 - \ldots\right],\\
\varepsilon &= P(t)\left[1 - R_2(t)x^2 - R_4(t)x^4 - R_6(t)x^6 - \ldots\right],\\
u &= M(t)\left[1 - N_2(t)x^2 - N_4(t)x^4 - N_6(t)x^6 - \ldots\right].
\end{aligned} \tag{2}$$

Here A, P and M are the amplitudes, expectedly maximum values of the functions reached in the middle of the jet, $x = 0$. The structure functions in the square brackets describe the dome-like profiles descending from the maxima down to zero at $x = h(t)$.

Substituting (2) into the dynamic equations (1) and collecting terms with same powers of x gives the system of ODEs

$$\begin{aligned}
\dot{A} &= -\alpha_1\frac{2A^3B_2}{P} - \alpha_3 P\,,\\
\dot{P} &= -\beta_1 2A^2R_2 - \beta_3\frac{P^2}{A}\,,\\
\dot{M} &= -\chi\frac{2A^2MN_2}{P}\,,\\
\dot{B}_2 &= -\alpha_1\frac{10A^2B_2^2}{P} + \alpha_3\frac{PB_2}{A} + \alpha_1\frac{6A^2B_2R_2}{P}\\
&\quad +\alpha_1\frac{12A^2B_4}{P} - \alpha_2\frac{4AM^2N_2^2}{P} - \alpha_3\frac{PR_2}{A}\,,\\
\dot{R}_2 &= -\beta_1\frac{12A^2B_2R_2}{P} + \beta_1\frac{8A^2R_2^2}{P} - \beta_3\frac{PR_2}{A}\\
&\quad +\beta_1\frac{12A^2R_4}{P} - \beta_2\frac{4AM^2N_2^2}{P} + \beta_3\frac{PB_2}{A}\,,\\
\dot{N}_2 &= -\chi\frac{12A^2B_2N_2}{P} + \chi\frac{2A^2N_2^2}{P} + \chi\frac{6A^2N_2R_2}{P}\\
&\quad +\chi\frac{12A^2N_4}{P}\,,
\end{aligned} \tag{3}$$

$$
\begin{aligned}
\dot{B}_4 &= -\alpha_1 \frac{58A^2B_2B_4}{P} + \alpha_3 \frac{PB_4}{A} + \alpha_1 \frac{10A^2B_2^3}{P} \\
&\quad -\alpha_1 \frac{20A^2B_2^2R_2}{P} + \alpha_1 \frac{10A^2B_2R_2^2}{P} + \alpha_1 \frac{10A^2B_2R_4}{P} \\
&\quad +\alpha_1 \frac{20A^2B_4R_2}{P} + \alpha_1 \frac{30A^2B_6}{P} + \alpha_2 \frac{8AB_2M^2N_2^2}{P} \\
&\quad -\alpha_2 \frac{4AM^2N_2^2R_2}{P} - \alpha_2 \frac{16AM^2N_2N_4}{P} - \alpha_3 \frac{PR_4}{A}, \\
\dot{R}_4 &= -\beta_1 \frac{40A^2B_2R_4}{P} + \beta_1 \frac{2A^2R_2R_4}{P} - \beta_3 \frac{PR_4}{A} \\
&\quad +\beta_1 \frac{10A^2B_2^2R_2}{P} - \beta_1 \frac{20A^2B_2R_2^2}{P} - \beta_1 \frac{20A^2B_4R_2}{P} \\
&\quad +\beta_1 \frac{10A^2R_2^3}{P} + \beta_1 \frac{30A^2R_2R_4}{P} + \beta_1 \frac{10A^2R_2^3}{P} \\
&\quad +\beta_1 \frac{30A^2R_2R_4}{P} + \beta_1 \frac{30A^2R_6}{P} + \beta_2 \frac{4AB_2M^2N_2^2}{P} \\
&\quad -\beta_2 \frac{16AM^2N_2N_4}{P} + \beta_3 \frac{B_2^2P}{A} - \beta_3 \frac{2B_2PR_2}{A} \\
&\quad +\beta_3 \frac{B_4P}{A} + \beta_3 \frac{PR_2^2}{A}, \\
\dot{N}_4 &= -\chi \frac{40A^2B_2N_4}{P} + \chi \frac{2A^2N_2N_4}{P} + \chi \frac{10A^2B_2^2N_2}{P} \\
&\quad -\chi \frac{20A^2B_2N_2R_2}{P} - \chi \frac{20A^2B_4N_2}{P} + \chi \frac{10A^2N_2R_2^2}{P} \\
&\quad +\chi \frac{10A^2N_2R_4}{P} + \chi \frac{20A^2N_4R_2}{P} + \chi \frac{30A^2N_6}{P}, \\
&\ldots
\end{aligned}
\tag{4}
$$

Among possible closure assumptions we choose that that satisfies the physical requirement that the fronts of the turbulent energy, dissipation rate and momentum coincide at all times. By the physics of diffusion, if the fronts are different initially, they should quickly catch up with each other. Consider a notional situation when the momentum front is initially behind the energy and dissipation-rate front (we suppose that these two coincide). Then the turbulent diffusion will instantaneously transfer the momentum forward up to the energy/dissipation-rate front position. Conversely, if the momentum front is initially ahead of the energy/dissipation-rate front, it will stay motionless for some time since there is no turbulence in the vicinity. The momentum front will move only when the energy/dissipation front catches up, after which the fronts will move together.

Thus, we require that K, ε and u turn into zero at the same location $x = h(t)$. Taking into account the terms up to the 4th order in (2) we have

$$
\begin{aligned}
1 - B_2h^2 - B_4h^4 &= 0, \\
1 - R_2h^2 - R_4h^4 &= 0, \\
1 - N_2h^2 - N_4h^4 &= 0.
\end{aligned}
\tag{5}
$$

The front equations (5) are complemented by the truncated dynamic equations (3),

$$
\begin{aligned}
\dot{A} &= -\alpha_1 \frac{2A^3B_2}{P} - \alpha_3 P, \\
\dot{P} &= -\beta_1 2A^2R_2 - \beta_3 \frac{P^2}{A}, \\
\dot{M} &= -\chi \frac{2A^2MN_2}{P}, \\
\dot{B}_2 &= -\alpha_1 \frac{10A^2B_2^2}{P} + \alpha_3 \frac{PB_2}{A} + \alpha_1 \frac{6A^2B_2R_2}{P} + \alpha_1 \frac{12A^2B_4}{P} \\
&\quad -\alpha_2 \frac{4AM^2N_2^2}{P} - \alpha_3 \frac{PR_2}{A}, \\
\dot{R}_2 &= \beta_1 \frac{8A^2R_2^2}{P} - \beta_3 \frac{PR_2}{A} - \beta_1 \frac{12A^2B_2R_2}{P} + \beta_1 \frac{12A^2R_4}{P} \\
&\quad -\beta_2 \frac{4AM^2N_2^2}{P} + \beta_3 \frac{PB_2}{A}, \\
\dot{N}_2 &= \chi \frac{2A^2N_2^2}{P} - \chi \frac{12A^2B_2N_2}{P} + \chi \frac{6A^2N_2R_2}{P} + \chi \frac{12A^2N_4}{P}, \\
\dot{B}_4 &= -\alpha_1 \frac{58A^2B_2B_4}{P} + \alpha_3 \frac{PB_4}{A} + \alpha_1 \frac{10A^2B_2^3}{P} \\
&\quad -\alpha_1 \frac{20A^2B_2^2R_2}{P} + \alpha_1 \frac{10A^2B_2R_2^2}{P} + \alpha_1 \frac{10A^2B_2R_4}{P} \\
&\quad +\alpha_1 \frac{20A^2B_4R_2}{P} + \alpha_1 \frac{30A^2B_6}{P} + \alpha_2 \frac{8AM^2N_2^2B_2}{P} \\
&\quad -\alpha_2 \frac{4AM^2N_2^2R_2}{P} - \alpha_2 \frac{16AM^2N_2N_4}{P} - \alpha_3 \frac{P^2R_4}{AP}.
\end{aligned}
\tag{6}
$$

The system (5)–(6) contains 10 equations with respect to 10 unknowns: A, P, M, B_2, R_2, N_2, B_4, R_4, N_4 and h, all depending on t.

Introduce the new time τ by

$$
\frac{d}{\left(A^2B_2/P\right)\, dt} = \frac{d}{d\tau} \equiv ()' \tag{7}
$$

and divide (6) by A^2B_2/P. This conveniently transforms (6) into the form with linear terms:

$$
\begin{aligned}
A' &= -\alpha_1 2A - \alpha_3 \frac{P^2}{A^2B_2}, \\
P' &= -\beta_1 \frac{2R_2P}{B_2} - \beta_3 \frac{P^3}{A^3B_2}, \\
M' &= -\chi \frac{2MN_2}{B_2}, \\
{B_2}' &= -\alpha_1 10B_2 + \alpha_3 \frac{P^2}{A^3} + \alpha_1 6R_2 + \alpha_1 \frac{12B_4}{B_2} \\
&\quad -\alpha_2 \frac{4M^2N_2^2}{AB_2} - \alpha_3 \frac{P^2R_2}{A^3B_2}, \\
{R_2}' &= -\beta_1 12R_2 + \beta_1 \frac{8R_2^2}{B_2} - \beta_3 \frac{P^2R_2}{A^3B_2} + \beta_1 \frac{12R_4}{B_2} \\
&\quad -\beta_2 \frac{4M^2N_2^2}{AB_2} + \beta_3 \frac{P^2}{A^3}, \\
{N_2}' &= -\chi 12N_2 + \chi \frac{2N_2^2}{B_2} + \chi \frac{6N_2R_2}{B_2} + \chi \frac{12N_4}{B_2},
\end{aligned}
\tag{8}
$$

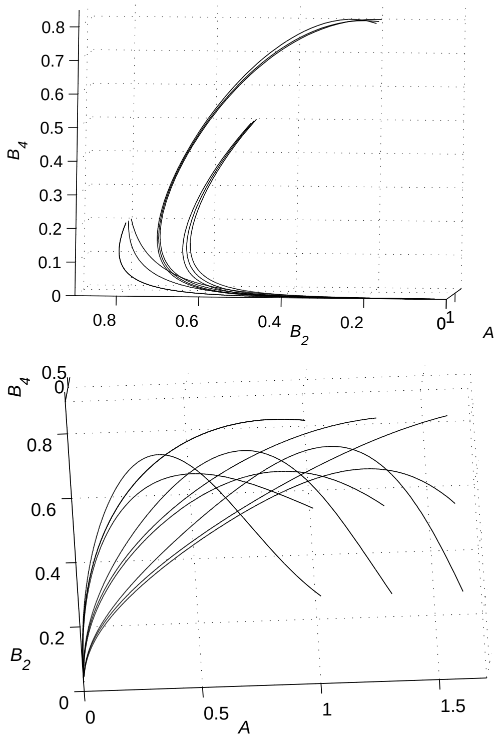

Figure 1: Trajectories (different views) in the space of the energy variables.

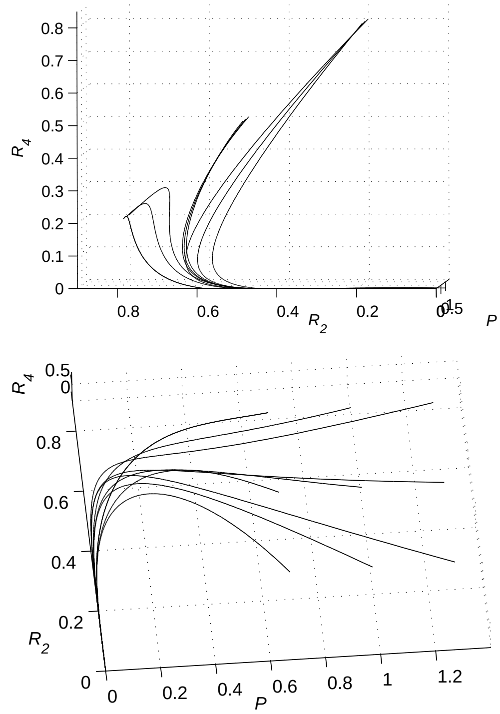

Figure 2: Trajectories (different views) in the spaces of the dissipation-rate variables.

$$
\begin{aligned}
{B_4}' = {} & -\alpha_1 58 B_4 + \alpha_3 \frac{P^2 B_4}{A^3 B_2} + \alpha_1 10 B_2^2 - \alpha_1 20 B_2 R_2 \\
& + \alpha_1 10 R_2^2 + \alpha_1 10 R_4 + \alpha_1 \frac{20 B_4 R_2}{B_2} + \alpha_1 \frac{30 B_6}{B_2} \\
& + \alpha_2 \frac{8 M^2 N_2^2}{A} - \alpha_2 \frac{4 M^2 N_2^2 R_2}{A B_2} - \alpha_2 \frac{16 M^2 N_2 N_4}{A B_2} \\
& - \alpha_3 \frac{P^2 R_4}{A^3 B_2} .
\end{aligned} \tag{9}
$$

Numerical solutions of the system (5), (8), (9) are displayed in Fig. 1–3. We used $\alpha_1 = 0.09$, $\alpha_2 = 0.09$, $\alpha_3 = 1$, $\beta_1 = 0.07$, $\beta_2 = 0.13$, $\beta_3 = 1.92$, $\chi = 0.09$. The initial positions of the energy front, dissipation-rate front and velocity front coincided.

From the Figures we observe that some variables are fast and some are slow. The amplitudes A and P decay rapidly in comparison to B_2 and R_2. This decay is largely due to the terms with α_3 and β_3, linked to the energy dissipation rate. The velocity amplitude M, compared to N_2, decays not as rapidly though. The variables B_4, R_4 and N_4 (and higher-order variables) decay rapidly compared to B_2, R_2 and N_2. Thus, the variables B_2, R_2 and N_2 are slow.

Notice that, except in the amplitude equations (8) the fast variables A, P and the variable M appear in the right-hand sides only in ratios P^2/A^3 and A/M^2. We anticipate, and confirm later in the paper, that these ratios are slow. We define

$$
E = \frac{P^2}{A^3} , \quad S = \frac{A}{M^2} . \tag{10}
$$

Differentiating (10) and expressing the derivatives A', P' and M' from (8) we deduce the dynamic equations for E and S. Also, we add the dynamic equation for N_4 so that all the 4th order variables, B_4, R_4 and N_4, now evolve according to their respective dynamic laws. We obtain

$$
\begin{aligned}
S' &= -\alpha_1 2 S - \alpha_3 \frac{ES}{B_2} + \chi 4 \frac{S N_2}{B_2} , \\
E' &= -\beta_1 4 \frac{R_2 E}{B_2} + \alpha_1 6 E + (3\alpha_3 - 2\beta_3) \frac{E^2}{B_2} , \\
{B_2}' &= -\alpha_1 10 B_2 + \alpha_3 E + \alpha_1 6 R_2 + \alpha_1 \frac{12 B_4}{B_2} \\
& \qquad - \alpha_2 \frac{4 N_2^2}{S B_2} - \alpha_3 \frac{E R_2}{B_2} , \\
{R_2}' &= -\beta_1 12 R_2 + \beta_1 \frac{8 R_2^2}{B_2} + \beta_3 \frac{E R_2}{B_2} + \beta_1 \frac{12 R_4}{B_2} \\
& \qquad - \beta_2 \frac{4 N_2^2}{S B_2} + \beta_3 E - \beta_3 \frac{2 E R_2}{B_2} , \\
{N_2}' &= -\chi 12 N_2 + \chi \frac{2 N_2^2}{B_2} + \chi \frac{6 N_2 R_2}{B_2} + \chi \frac{12 N_4}{B_2} , \\
{B_4}' &= -\alpha_1 58 B_4 + \alpha_3 \frac{E B_4}{B_2} + \alpha_1 10 B_2^2 - \alpha_1 20 B_2 R_2 \\
& \qquad + \alpha_1 10 R_2^2 + \alpha_1 10 R_4 + \alpha_1 \frac{20 B_4 R_2}{B_2} + \alpha_1 \frac{30 B_6}{B_2} \\
& \qquad + \alpha_2 \frac{8 N_2^2}{S} - \alpha_2 \frac{4 N_2^2 R_2}{S B_2} - \alpha_2 \frac{16 N_2 N_4}{S B_2} - \alpha_3 \frac{E R_4}{B_2} ,
\end{aligned} \tag{11}
$$

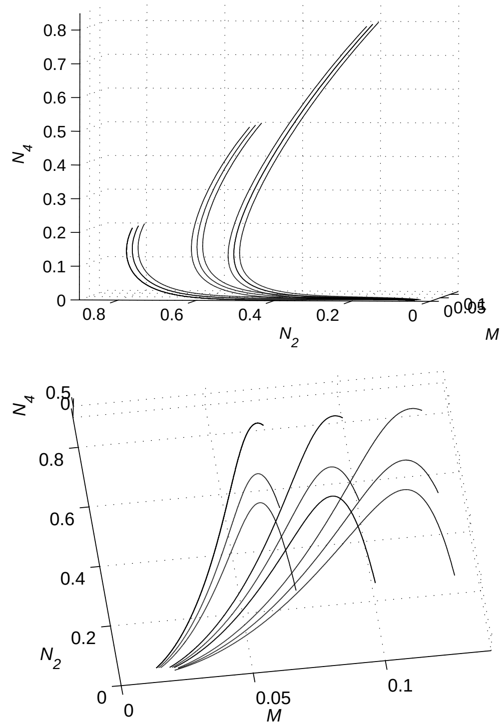

Figure 3: Trajectories (different views) in the space of the velocity variables.

$$
\begin{aligned}
R_4{}' &= -\beta_1 40 R_4 + \beta_1 2\frac{R_2 R_4}{B_2} + \beta_3 \frac{E R_4}{B_2} \\
&\quad + \beta_1 10 B_2 R_2 - 20\beta_1 R_2^2 - \beta_1 20 \frac{R_2 B_4}{B_2} + \beta_1 10 \frac{R_2^3}{B_2} \\
&\quad + \beta_1 30 \frac{R_2 R_4}{B_2} + \beta_1 30 \frac{R_6}{B_2} + \beta_2 4 \frac{N_2^2}{S} \\
&\quad - \beta_2 16 \frac{N_2 N_4}{S B_2} + \beta_3 E B_2 - \beta_3 2 E R_2 + \beta_3 \frac{E B_4}{B_2} \\
&\quad + \beta_3 \frac{E R_2^2}{B_2} - \beta_3 2 \frac{E R_4}{B_2}\,, \\
N_4{}' &= -\chi 40 N_4 + \chi 2 \frac{N_2 N_4}{B_2} + \chi 10 B_2 N_2 - \chi 20 N_2 R_2 \\
&\quad - \chi 20 \frac{N_2 B_4}{B_2} + \chi 10 \frac{N_2 R_2^2}{B_2} + \chi 10 \frac{N_2 R_4}{B_2} \\
&\quad + \chi 20 \frac{R_2 N_4}{B_2}\,.
\end{aligned}
\tag{12}
$$

The dynamical system (11)–(12) is augmented to the closed form by the front equations

$$
\begin{aligned}
&1 - B_2 h^2 - B_4 h^4 - B_6 h^6 = 0\,, \\
&1 - R_2 h^2 - R_4 h^4 - R_6 h^6 = 0\,, \\
&1 - N_2 h^2 - N_4 h^4 = 0\,.
\end{aligned}
\tag{13}
$$

Fig. 4 demonstrates that E, S and B_2 behave linearly against each other and therefore can be identified as slow variables.

Notice a spectral gap between the linear decay rates in (12): the coefficient at B_4, $(-58\alpha_1)$, is about 5 times larger than the coefficient at B_2, $(-10\alpha_1)$, at R_2, $(-12\beta_1)$, and at N_2, (-12χ). The numerical experiments show that the linear terms dominate on early stages of the dynamics forcing B_4, R_4 and N_4 to decay. Accordingly, the linear terms quickly drop to a level comparable to the rest of the terms.

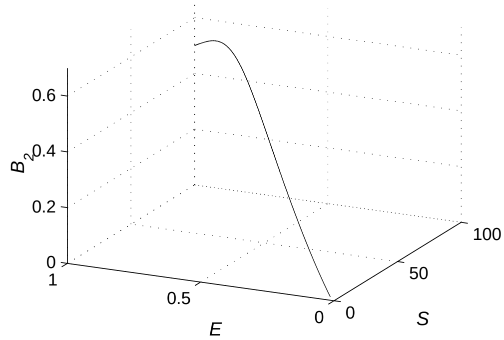

Figure 4: The behaviour of the slow variables.

Simple example of an attractor

This behaviour resembles the dynamics near attractors called centre manifolds. A centre manifold attracts trajectories of a dynamical system where some, slow, variables have zero linear decay rates, while the other, fast, variables have negative linear decay rates [2]. We illustrate this on a simple example from [7]:

$$
\begin{aligned}
\dot{x} &= -px - xy\,, \\
\dot{y} &= -y + x^2 - 2y^2\,.
\end{aligned}
\tag{14}
$$

If $p = 0$, then it can be shown that the attractor is precisely

$$
y = x^2\,. \tag{15}
$$

Driven by the linear term $(-y)$ the variable y quickly drops and trajectories fall onto the attracting manifold (15) on which the nonlinear terms $(x^2 - 2y^2)$ are comparable to the linear term $(-y)$. Observe that the variable y depends on t via the slow variable x.

If p is positive but relatively small, the attracting manifold can be found as a perturbation of (15). The case of small $p > 0$ is similar to our situation in (12).

Remarkably, in the unperturbed case $p = 0$ the attractor (15), in its leading order, can be obtained by simply replacing the time derivative $\dot{y}$ by zero: $0 = -y + x^2 - 2y^2$ giving $y = x^2 + o(x^2) \to x^2$ when $x \to 0$. The motion on the attractor is obtained from the first equation (14). In the leading order $\dot{x} = -x^3$.

If $p > 0$, then, strictly speaking, the derivative $\dot{y}$ must be taken into account. However, if p is small enough, that is the spectral gap between the linear decay rate 1 of y and p of x is considerable, then $y = x$ can acceptably approximate the attractor.

Attractor for the turbulent jet

We take the similar approach in our turbulence problem.

Replace in (11)–(13) the time derivatives of B_4, R_4 and N_4 by zeroes. This gives 6 algebraic equations to determine the 6 variables: B_4, R_4, N_4, B_6, R_6 and h in terms of the slow variables E,

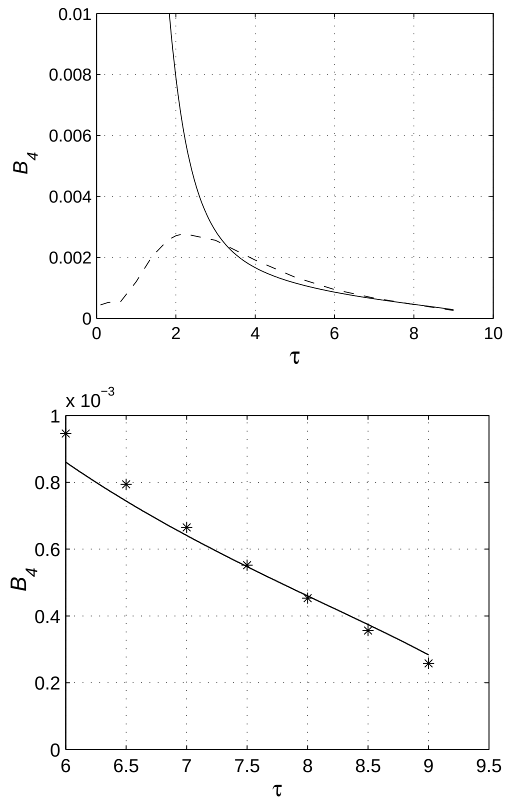

Figure 5: Actual behaviour of B_4 (solid line) and its projection onto the attractor. End part of the curve is zoomed.

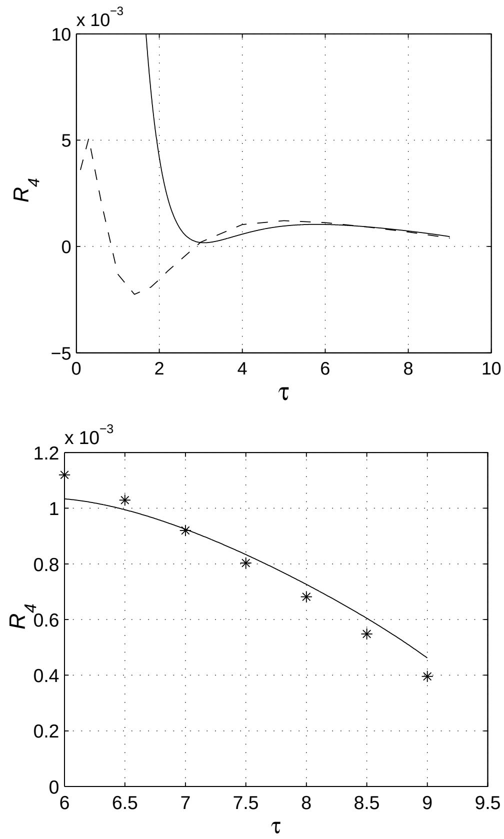

Figure 6: Actual behaviour of R_4 (solid line) and its projection.

S, B_2, R_2 and N_2:

$$
\begin{aligned}
0 &= 1 - B_2h^2 - B_4h^4 - B_6h^6\,,\\
0 &= 1 - R_2h^2 - R_4h^4 - R_6h^6\,,\\
0 &= 1 - N_2h^2 - N_4h^4\,,\\
0 &= -\alpha_1 58B_4 + \alpha_3\frac{EB_4}{B_2} + \alpha_1 10B_2^2 - \alpha_1 20B_2R_2\\
&\quad +\alpha_1 10R_2^2 + \alpha_1 10R_4 + \alpha_1\frac{20B_4R_2}{B_2} + \alpha_1\frac{30B_6}{B_2}\\
&\quad +\alpha_2\frac{8N_2^2}{S} - \alpha_2\frac{4N_2^2R_2}{SB_2} - \alpha_2\frac{16N_2N_4}{SB_2} - \alpha_3\frac{ER_4}{B_2}\,,\\
0 &= -\beta_1 40R_4 + \beta_1 2\frac{R_2R_4}{B_2} + \beta_3\frac{ER_4}{B_2} + \beta_1 10B_2R_2 \qquad (16)\\
&\quad -20\beta_1R_2^2 - \beta_1 20\frac{R_2B_4}{B_2} + \beta_1 10\frac{R_2^3}{B_2} + \beta_1 30\frac{R_2R_4}{B_2}\\
&\quad +\beta_1 30\frac{R_6}{B_2} + \beta_2 4\frac{N_2^2}{S} - \beta_2 16\frac{N_2N_4}{SB_2} + \beta_3 EB_2\\
&\quad -\beta_3 2ER_2 + \beta_3\frac{EB_4}{B_2} + \beta_3\frac{ER_2^2}{B_2} - \beta_3 2\frac{ER_4}{B_2}\,,\\
0 &= -\chi 40N_4 + \chi 2\frac{N_2N_4}{B_2} + \chi 10B_2N_2 - \chi 20N_2R_2\\
&\quad -\chi 20\frac{N_2B_4}{B_2} + \chi 10\frac{N_2R_2^2}{B_2} + \chi 10\frac{N_2R_4}{B_2} + \chi 20\frac{R_2N_4}{B_2}\,.
\end{aligned}
$$

We solved system (16) numerically and compared typical trajectories: a trajectory obtained from the full system (11)–(13) and a trajectory obtained as described above where the values of the slow variables are taken from the solution of the full system. The latter trajectory therefore constitutes the projection of the actual trajectory onto an attractor.

The comparison is shown in Fig. 5–7. For the energy and dissipation-rate variables the actual solution curve approaches its projection very closely. For the velocity variables the actual curve and its projection are also close although to a lesser extent. Overall, the attraction is quite evident.

The higher-order coefficients of series (2), B_i, R_i and N_i for $i = 6, 8, \ldots$, can be expressed through the slow variables E, S, B_2, R_2 and N_2 in the similar way as B_4, R_4 and N_4 above. As new equations are added into the algebraic system (16), more terms are to be added in the front equations (13). As a result, any number of the coefficients of the series (2) can be determined as implicit functions of the slow variables; such functions would constitute the sought attractor.

Conclusions

We analysed the K–ε model of the expanding turbulent jet shaped as a plane layer. The profiles of energy, dissipation rate and velocity across the jet are sought in the form of power series. The series coefficients satisfy a nonlinear dynamical system with a few slow variables. Using these variables, we found an approximate form of attractor in the form of a system of algebraic equations connecting higher-order variables and slow variables. The convergence of the trajectories to the attractor is demonstrated.

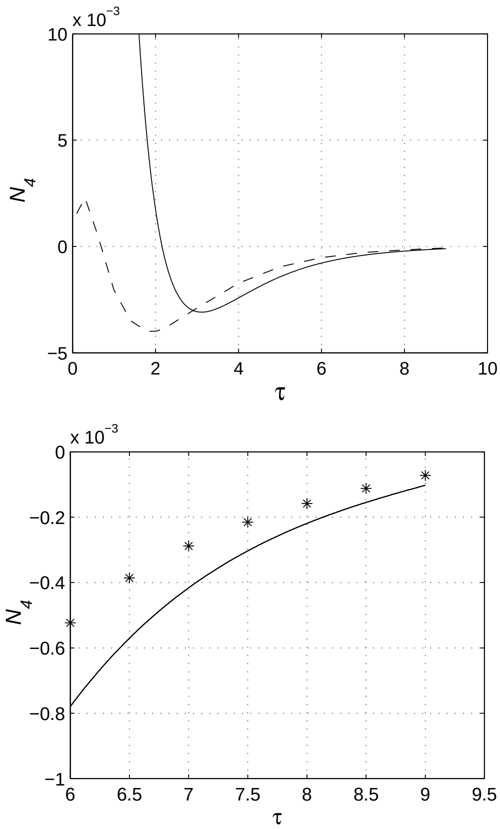

Figure 7: Actual behaviour of N_4 (solid line) and its projection.

References

[1] Bradbury, L.J.S., The Structure of A Self-preserving Turbulent Plane Jet, *J. Fluid Mech.*, **23**, 1965, 31–64.

[2] Carr, J., Applications of Centre Manifold Theory, *Applied Mathematical Sciences*, **35**, Springer–Verlag, 1981.

[3] Crow, S.C. and Champagne, F.H., Orderly Structure in Jet Turbulence, *J. Fluid Mech.*, **48**, 1971, 547–591.

[4] Hanjalic, K. and Launder, B.E., A Reynolds Stress Model of Turbulence and Its Applications to Thin Shear Flows, *J. Fluid Mech.*, **52**, 1972, 609–638.

[5] Launder, B.E., Reece, G.J. and Rodi, W., Progress in The Development of A Reynolds-stress Turbulence Closure, *J. Fluid Mech.*, **68**, 1975, 537–566.

[6] Polyanin, A.D. and Zaitsev, V.F., *Handbook of Nonlinear Partial Differential Equations*, Chapman and Hall/CRC, 2004.

[7] Roberts, A.J., Appropriate Initial Conditions for Asymptotic Descriptions of The Long Term Evolution of Dynamical Systems, *J. Austral. Math. Soc. Ser. B*, **31**, 1989, 48–75.

[8] Strunin, D.V. and Roberts, A.J., Self-similarity of Decaying Turbulent Jet, *Proc. of the 5th Eng. Math. and Applic. Conf. EMAC-2002*, Eds. Pemberton, M., Turner, I. and Jacobs, P., The Inst. of Engineers, Brisbane, Australia, 205–210.

[9] Wygnanski, I. and Fiedler, H.E., Some Measurements in the Self-preserving Jet, *J. Fluid Mech.*, **38**, 1969, 577–612.

[10] Zel'dovich, Ya.B. and Kompaneets, A.S., On the Theory of Heat Propagation for Temperature Dependent Thermal Conductivity. *Collection Commemorating the 70th Anniversary of A.F. Joffe*, Izv. Akad. Nauk SSSR, 1950.